

# Microfabricated ZSM-5 zeolite micromembranes

Yat Lai Adrian Leung, K.L. Yeung\*

Department of Chemical Engineering, The Hong Kong University of Science and Technology, Clear Water Bay, Kowloon, Hong Kong

Received 8 March 2004

## Abstract

Free-standing microfabricated (MFI) zeolite micromembranes were successfully fabricated on a silicon substrate. Three zeolites including Sil-1, ZSM-5 (Si/Al = 60) and ZSM-5 (Si/Al = 40) were prepared. The zeolite micromembrane units were tested for gas permeation and separation. The micromembranes displayed an order of magnitude higher permeability (i.e., H<sub>2</sub> and He) compared to traditional supported zeolite membranes and possessed excellent permselectivity. Separation was conducted for a gas mixture containing hydrogen, methane and carbon dioxide. Zeolite chemistry plays a role in membrane separation. Sil-1 micromembrane selectively permeated the heavier hydrocarbon and carbon dioxide resulting in a hydrogen-enriched retentate stream, while hydrogen was concentrated at the permeate outlet of the ZSM-5 micromembrane.

© 2004 Elsevier Ltd. All rights reserved.

*Keywords:* Nanoporous material; Miniature membrane; Microseparator; Gas permeation; Gas separation

## 1. Introduction

Miniaturization can benefit many chemical processes including reaction and separation. One obvious advantage is that an enormous surface area could be accommodated in a small, compact volume in a microsystem. The large surface area and small fluid volume result in better mass and heat transfer properties. However, the most important contribution of a miniature microfabricated chemical device is the unprecedented opportunity to control and manipulate the contact and mixing between well-defined fluid elements to attain a more efficient performance. Indeed, it has been predicted that the miniature chemical system will play a key role in the realization of a distributed chemical production where on-site and on-demand, clean production will be fulfilled in environmentally responsible and safe conditions (Worz, 2001). Various research groups had made significant advances in the design, fabrication and testing of microchemical systems, in particular, microreactors. Works by Ajmera and Jensen (2001), Chambers and Sandford (2001),

Haswell and Watts (2003), Wan et al. (2003), Lai et al. (2003) and Kolb and Hessel (2004) are good examples of the use of microreactor technology for safe and clean production of high-value fine chemicals. Review articles by Gavriilidis et al. (2002), Hessel and Lowe (2003) and Jahnisch et al. (2004) discuss the recent trend in microreactor research.

Today, many miniature chemical devices such as microreactors, micromixers and microseparators are integral components of “laboratory-on-a-chip”. These devices have an enormous potential as analytical tools for chemical, biochemical and biomedical researches. They also have immediate application as diagnostic tools for rapid screening of diseases. The last few years have witnessed an increasing demand for portable energy source to power our increasingly mobile lifestyle. Man-portable electronic devices such as mobile phones, personal digital assistants and laptop computers are becoming smaller, faster and more sophisticated, putting a premium on small, lightweight energy devices that could reliably supply their greater energy needs. This has spurred research in micro fuel cell and related technologies in miniature fuel reformers and converters. Micro-fuel cell has the advantages of high specific and volumetric energy densities, longer life cycle, zero-recharging time, greater

\* Corresponding author. Tel.: +852 2358 7123; fax: +852 2358 0054.  
E-mail address: kekyeung@ust.hk (K.L. Yeung).

flexibility and absence of hazardous waste products at the end of the life cycle.

It was acknowledged that microscale separation is one of the core technologies that needs to be developed for the microchemical system whether for use in future miniature chemical plants or today's lab-on-a-chip device. Most separation processes can benefit directly from the large surface area-to-volume ratio that can be obtained in a microseparator. In fact, a few separation processes, such as extraction and membrane separation, have been successfully miniaturized. There is a growing interest in the application of miniature transport membranes in sensors, microseparators and microreactors, as well as component parts of a lab-on-a-chip microdevices. Most of the research on micromembranes focuses on palladium and polymer materials. These are exemplified by the work of Quiram and Jensen (2000), Karnik et al. (2003), Kusakabe et al. (2001), Cui et al. (2000), Schiewe et al. (2001) and Martin et al. (1999). Hydrogen separation and purification from both gas and reaction mixtures were successfully conducted in palladium micromembranes. Schiewe and coworkers (2001) employed a polymeric membrane in a microreactor to enrich the ethylene oxide product from ethylene epoxidation. Martin et al. (1999) used a porous polyimide membrane in a microchannel liquid–liquid contactor to transport dissolved 1-hexanol between hexane and water solvents. Mesoporous alumina and silica membranes made by anodization were also used as membrane contactors in the miniature separation device (Haswell and Skelton, 2000).

This work reports the fabrication of three MFI zeolite micromembranes with different Si/Al ratios of 40, 60 and  $\infty$ . The micromembrane units were characterized and tested for gas permeation and separation. Although there are numerous works that discuss the fabrication of zeolite micromembranes, to our knowledge this is the first successful demonstration of gas permeation and separation in zeolite micromembrane.

## 2. Experiment

### 2.1. Fabrication of zeolite micromembrane

The zeolite micromembranes were made using the traditional semiconductor fabrication method. It has the advantage of being a mature technology with a well-established fabrication protocol and a global manufacturing infrastructure in the form of semiconductor foundries. In addition, many of the microfluidic devices, microelectromechanical systems (MEMS), sensors and smart circuitry that are essential components in a chemical microsystem are made by the traditional microfabrication method (Madou, 1997). A common fabrication technology is expected to simplify and facilitate the integration of various working components' structure and function into an operational chemical microdevice. The procedure for making zeolite micromembranes involves

three steps: (1) the fabrication of support structure, (2) the synthesis of zeolite micromembrane and (3) membrane activation.

The support structure for a micromembrane array was etched into the silicon substrate using the traditional semiconductor fabrication method. Four-inch, p-type (100) silicon wafers purchased from JXC were cleaned and stripped of native oxide layer before coating both sides of the wafer with a 500 nm thick, low-stress silicon nitride ( $\text{Si}_3\text{N}_4$ ) layer. Four micrometer thick layers of HR207 photoresist were spin-coated on both sides of the wafer and soft baked at 378 K for 30 min. Two separate masks were needed to create the desired support structure: one containing a grid-like pattern consisting of  $7 \times 7$  array of 300  $\mu\text{m}$  squares and the other was a single large rectangular pattern. The patterns from the two masks were transferred simultaneously onto the wafer by standard lithography process involving UV exposure and resist development. The exposed silicon nitrides were removed by dry etching to uncover the silicon substrate underneath. The remaining photoresists were stripped using oxygen plasma, before the wafer was etched in a bath containing 30% potassium hydroxide (BDH Lab) at 353 K. Strict temperature regulation and good mixing are essential for creating a uniformly etched pattern. The wafer was etched until only a thin layer ( $\sim 50 \mu\text{m}$ ) of silicon separated the two patterns. Each step of the fabrication process was inspected by an optical microscope (Olympus BH-2) to ensure good reproducibility. A scanning electron microscope (SEM, JEOL 6300f) was used to obtain the exact dimensions of the fabricated silicon support structure.

The synthesis of zeolite micromembranes involves pre-seeding of the silicon substrate with zeolite nanocrystals, followed by zeolite crystallization and growth under hydrothermal condition. The nanometer-sized zeolite seeds were prepared from a synthesis mixture containing 15 g fumed silica (0.01  $\mu\text{m}$ , 99.8%, Aldrich) and 0.85 g sodium hydroxide (98%, BDH) dissolved in 60 ml of 1 M tetrapropylammonium hydroxide solution (TPAOH, 1 M, Aldrich). 100  $\pm$  20 nm-sized silicalite-1 (Sil-1) seeds were recovered by a series of centrifugation and rinsing steps after crystallization at 398 K for 8 h. A 5 wt% suspension of Sil-1 nanocrystals in ethanol (99.9%, Aldrich) was used for seeding. Selective seeding was achieved by grafting mercapto-3-propyltrimethoxysilanes (MPTS, 99%, Aldrich) onto the bare silicon surface of etched microcavities in the array. The grafted MPTS molecules anchor the zeolite seeds onto the silicon surface. Excess seeds deposited onto the surface of silicon nitride were removed using scotch tape and the sample was calcined in air at 823 K for 8 h. Inspections by optical and scanning electron microscopies were conducted to assess the quality of the seed coating prior to zeolite membrane growth.

The zeolite film was grown on the seeded surface of the microcavities by hydrothermal synthesis. Sil-1 and ZSM-5 zeolites were crystallized from synthesis solutions containing 40  $\text{SiO}_2$ : 0–1.6  $\text{Al}_2\text{O}_3$ : 0–10 NaOH: 1–10 TPAOH:

20,000 H<sub>2</sub>O. Calculated amounts of TPAOH and sodium hydroxide were first dissolved in 60 mL of distilled deionized water. The alumina precursor was prepared by reacting aluminum sulfate (98 + %, Aldrich) in excess ammonium hydroxide (28–30%, Fisher Scientific). A measured amount of alumina precursor was added to obtain zeolites with the desired Si/Al ratio. The silica source, tetraethyl orthosilicate (TEOS, 98%, Aldrich), was then added drop-by-drop with constant stirring. The solution was aged overnight to produce a clear and homogeneous synthesis solution. The seeded sample was positioned horizontally in a Teflon holder with the seeded pattern facing downward to prevent deposition of powder during the synthesis. The sample and synthesis solution were transferred into the Teflon bomb, sealed in a stainless-steel autoclave and placed in a preheated oven. The synthesis temperature and crystallization time were adjusted to obtain the membrane of desired thickness and crystallographic orientation. After rapid quenching, the sample was removed from the holder and rinsed with distilled deionized water to wash away any deposited powder. The structure, crystallinity and orientation of the deposited zeolites were analyzed by X-ray diffraction (XRD, Philips W 1030). The aluminum content was examined by X-ray photoelectron spectroscopy (XPS, Physical Electronics PHI 5600).

The final step in micromembrane preparation was membrane activation. This involved etching away the remaining 50  $\mu\text{m}$  silicon layer in tetramethylammonium hydroxide solution (TMAH, 25%, Moses Lake) to create the freestanding zeolite micromembranes. TMAH was chosen, since KOH can etch the zeolite. Care must be taken to regulate the etching rate to prevent nonuniform etching that can lead to pitting and undercutting. After etching, the micromembrane array was rinsed with distilled, deionized water to wash away excess TMAH and dried in an oven at 338 K. Leak test experiment was conducted using helium at a pressure difference of  $\Delta P = 400$  kPa to check the micromembrane unit for cracks and defects, before further treatment to remove the organic template molecules. A low-temperature ozone activation technique developed in our laboratory was employed for the organic template removal (Heng et al., 2004). The ozone treatment was conducted in a glass flow cell. The micromembrane-array unit was sandwiched between two halves of the flow cell, each containing a set of gas inlet and outlet. A gas mixture containing 100 ppm ozone was fed to the retentate-side of the flow cell, which was kept at a constant pressure of 135 kPa. The ozone gas was produced by an electrical discharge ozone generator (Trailigas, Ozonconcept OZC 1002) from high purity oxygen (99.7%, CWIG). The flow cell was heated at 1 K/min from room temperature to 373 K. During the ozone treatment, the flux through the membrane was monitored to establish the degree of membrane activation. The results were confirmed by the disappearance of the characteristic infrared signals of TPA-MFI as observed by a Fourier transform infrared microscope (Perkin-Elmer I-series FTIR microscope).

## 2.2. Gas permeation and separation

Gas permeation and separation experiments were conducted in a glass Wicke–Kallenbach cell. The micromembrane unit was sandwiched between two mating sections of the glass cell. Gases flow through the retentate compartment via a set of inlet and outlet ports. The gas flow was maintained above 250 sccm and the retentate pressure at 136 kPa. The experiments were carried out without sweep gas and the flux through the micromembranes was measured from the permeate outlet at ambient pressure (ca. 101.3 kPa). Helium (UHP), hydrogen (UHP), nitrogen (UHP), argon (UHP), methane (99.5%), and *n*-butane (99.9%) single gas permeances were tested at room temperature (ca. 300 K). The gases were purchased from CWIG and Hong Kong Specialty Gases and were purified through a series of moisture traps installed in the experimental setup. Prior to each experiment, the micromembrane unit was purged with helium at 403 K to remove adsorbed gases and moisture. Permeation measurements were made only after the steady-state flux of helium through the micromembrane reached the original value. The average permeance was calculated from three separate measurements. A gas mixture containing 61.7% hydrogen, 12.3% methane and 26.0% carbon dioxide was used in the separation study. The separation was carried out in the same experimental setup under identical conditions. The permeate was analyzed using an on-line gas chromatograph (HP 6890) equipped with thermal conductivity and flame ionization detectors in series and a CTR 1 column (Altech).

## 3. Results and discussion

### 3.1. Zeolite micromembrane

Fig. 1a displays a typical micromembrane unit. It consists of 49 zeolite micromembranes arranged in a square  $7 \times 7$  array on a silicon substrate. Each micromembrane resides in a fabricated cavity that acts as a temporary support. The selective seeding method confined the growth of zeolite layer within the interior surface of the fabricated cavities. Fig. 1b shows that the zeolite film does not grow on the unseeded silicon nitride layer that covers the surface of the micromembrane unit. This effectively isolated each micromembrane and prevented the accumulation of stresses that often led to failure in large membranes. Fig. 1c displays a cross-section of a zeolite-coated microcavity. The anisotropic etching produced cavities with walls sloping downward at an incline angle of  $54.7^\circ$  that terminated in a square bottom with sides measuring 260  $\mu\text{m}$ . The figure shows that the surface of the microcavity is uniformly coated with a thin layer of zeolite film. Grown from a monolayer seed (ca. 0.1–0.2  $\mu\text{m}$ ), the zeolites exhibit an anisotropic growth that gives the grains a distinct inverted pyramidal shape (Fig. 1d). X-ray diffraction analysis indicated that the zeolite film has a preferred

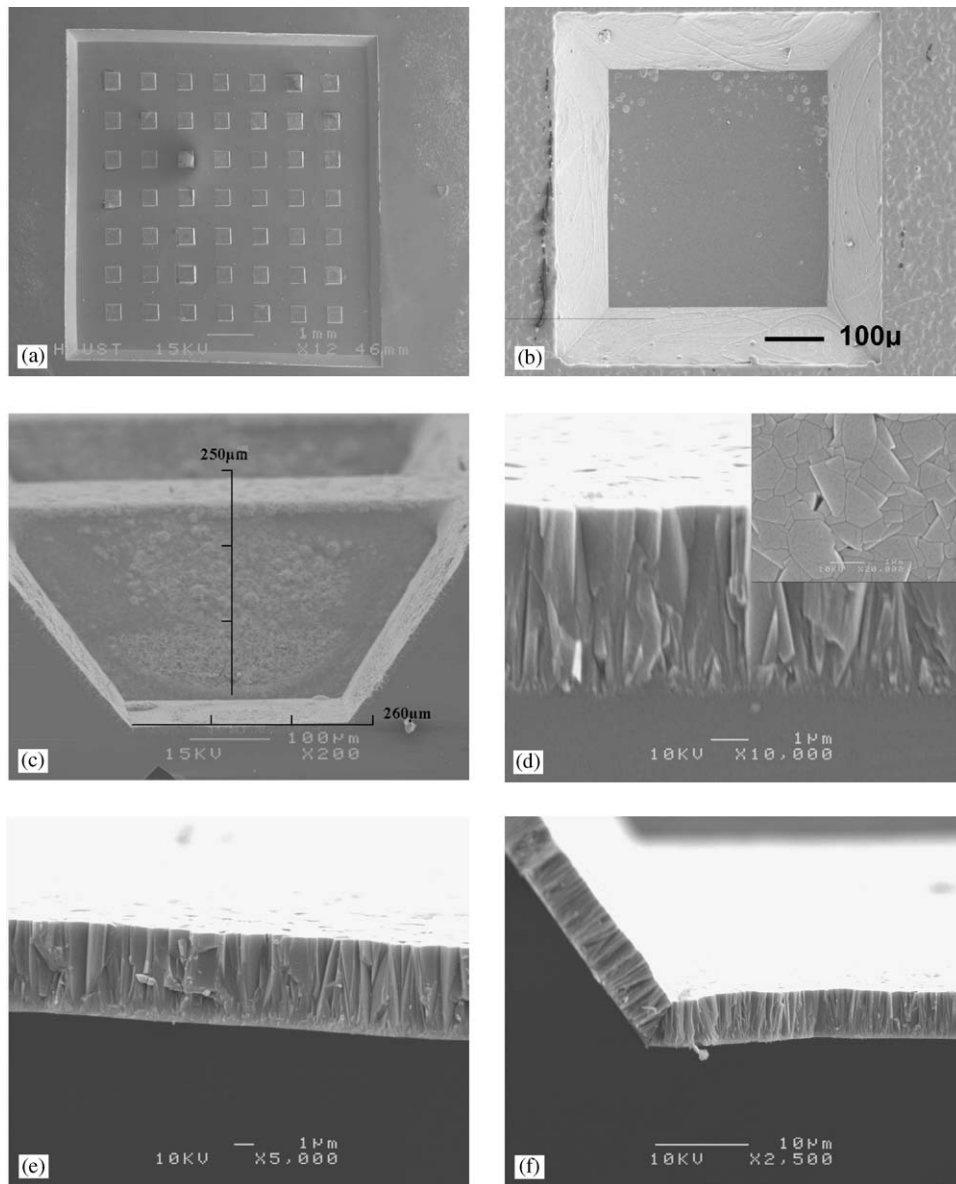


Fig. 1. (a) Scanning electron microscope picture of a micromembrane unit and (b) A higher magnification picture of a single micromembrane. (c) A cross-sectional view of the support structure after zeolite growth and before TMAH etching. The support structure consists of an array of microcavities etched into silicon. (d) A higher magnification picture of zeolite layer deposited onto the microcavity. An SEM picture of the zeolite surface is also included as an inset. (e) A freestanding zeolite micromembrane was obtained by etching away the remaining silicon, but excessive etching then results in the membrane shown in (f).

(101)—crystallographic orientation. Grain intergrowth is clearly evident from the film cross-section. An image of the film surface (Fig. 1d, inset) shows a mosaic of overlapping grains that have an average size of  $0.6 \mu\text{m}$ . A square meter of membrane area comprised of an estimated  $3.4 \times 10^{12}$  grains and the resulting grain boundary stretches to a length of  $8 \times 10^6 \text{ m}^2$  of membrane.

The thin layer of silicon (ca.  $50 \mu\text{m}$ ) was etched away to create the freestanding zeolite micromembrane shown in Fig. 1e. The  $5\text{-}\mu\text{m}$  zeolite film remained intact after the last of the supporting silicon layer was removed by selective etch-

ing with TMAH solution. The absence of flux during helium leak test indicated that the fabricated micromembranes were free of cracks and defects. The mechanical strength of the freestanding micromembranes was tested by increasing the helium gas pressure at the retentate at a rate of  $0.05 \text{ kPa/min}$  while maintaining the permeate pressure at ambient (ca.  $101.3 \text{ kPa}$ ). Experiments showed that Sil-1 and ZSM-5 micromembrane units are able to withstand a pressure difference of  $450 \text{ kPa}$ . Failure for the  $5\text{-}\mu\text{m}$  thick micromembrane (i.e., Sil-1 and ZSM-5 (Si/Al = 50) samples) occurred at a pressure difference of about  $500\text{--}600 \text{ kPa}$  and involved

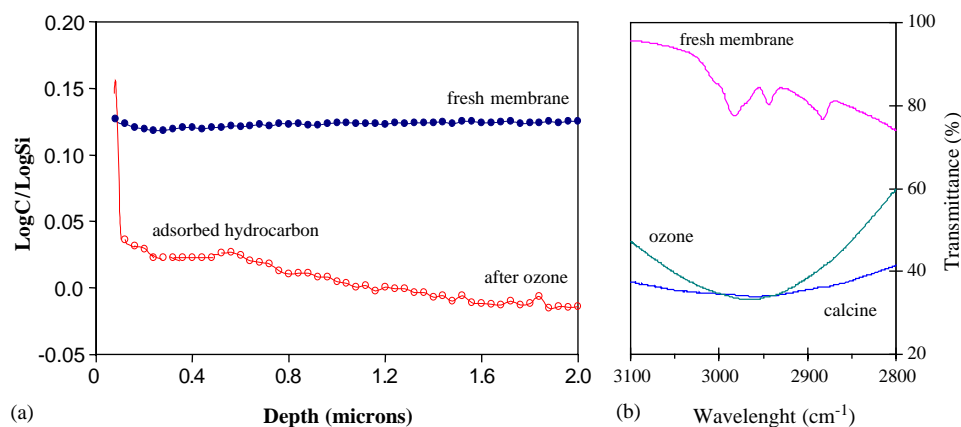


Fig. 2. (a) A plot of carbon-to-silicon signal across a Sil-1 micromembrane before and after ozone treatment. (b) Infrared signals for Sil-1 micromembrane before and after ozone treatment, as well as after air calcination.

the rupture of the free-standing membrane. Consistent results were obtained from repeated tests of the samples after the broken micromembranes were sealed with silver paste. SEM examination showed that membrane failure rarely involved more than one micromembrane and could take place anywhere within the  $7 \times 7$  micromembrane array. Failure propagation commonly observed in large zeolite membranes was absent in the tested units. This suggested that isolating the membrane into smaller individual units was effective in arresting the propagation of failure. The strength of the membrane was found to be independent of the aluminum content of the ZSM-5 zeolite, but increases in proportion to the membrane thickness. The supported membrane area (i.e., part of the micromembrane attached to the silicon wall) also affected the strength of the micromembrane. Overetching as shown in Fig. 1f weakened the micromembrane. Fig. 1f shows that the micromembrane possessed excellent intergrowth despite the large change in the membrane surface curvature. It also showed that zeolite growth orientation and crystal habit in relation to the supporting surface remained unchanged.

Organic template removal by high-temperature calcination often introduces defects and cracks in zeolites. This was observed even for micron-sized, single crystal zeolite particles (Geus and van Bekkum, 1995). It had been suggested that escaping gases formed during the decomposition of the organic template is responsible for the cracks in the zeolite crystals. Cracks are also common for calcined zeolite membranes and had been described by various authors (Dong et al., 2000; Tschaufeser and Parker, 1995). Although mismatched thermal expansion coefficient between support and membrane is an important factor, the rapid lattice contraction that accompanies the removal of the template molecule is believed to be the main cause of crack formation in supported zeolite membranes. In a separate experiment, ZSM-5 films (ca.  $5 \mu\text{m}$ ) were grown on silicon and were heat treated in air at 573, 673, 773 and 823 K. The samples were heated from room temperature at 0.5 K/min and cooled back down

at 1 K/min after 8 h of heat treatment. Analysis of the samples by infrared microscopy and SEM indicated that template removal was only significant at temperatures above 673 K and complete removal was obtained only at 823 K, but as treatment temperature increased the number of cracks increased rapidly. A low-temperature template removal method was employed for membrane activation to remedy this problem.

In a separate paper (Heng et al., 2004), we had shown that oxygen gas containing 100 ppm ozone could effectively remove the organic template from zeolite membranes in less than an hour at relatively mild temperatures (i.e., 373–423 K). Zeolite membranes treated by this method had fewer defects and possessed more reproducible permeation and separation properties. They also exhibited better permselectivity than a similar membrane calcined at higher temperature. The removal of the TPA molecules from a Sil-1 zeolite micromembrane unit was monitored using dynamic secondary ion mass spectrometer (dynamic-SIMS, Cameca IMS 4f) and infrared microscopy. Fig. 2a plots the carbon-to-silicon signal across the thickness of the zeolite membrane. The experiment was conducted using Cs microbeam source and the depth profiling of the sample was made by Ar sputtering at a rate of 50 nm/h. Due to time constraint, the dynamic-SIMS experiment was conducted only to a depth of  $2 \mu\text{m}$ . It is clear from the plot that the ozone treatment completely removed the TPA molecules from the zeolite pores. This was confirmed by the disappearance of the characteristic peaks of TPA-Sil-1 from infrared signals of the Sil-1 micromembrane after ozone treatment as shown in Fig. 2b.

### 3.2. Gas permeation and separation

Three zeolite micromembrane units were prepared and tested for gas permeation and separation. The synthesis composition and condition were adjusted so that the three test units consist of zeolites with different aluminum content (i.e., Si/Al =  $\infty$  for Sil-1; 40 and 60 for the two ZSM-5), but

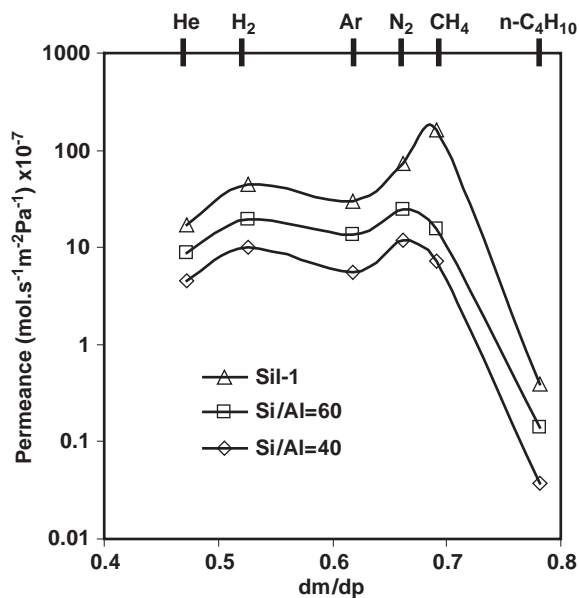


Fig. 3. Plots of single gas permeance as a function of  $dm/dp$  (i.e., the ratio of the kinetic diameter of the gas molecule and the average zeolite pore size (ca. 5.5 Å) for ZSM-5 micromembrane units with different aluminum content.

displayed similar membrane morphology and microstructure. All three test units had an average membrane thickness of  $5 \pm 0.3 \mu\text{m}$  and zeolite crystal size of  $0.6 \pm 0.4 \mu\text{m}$ . Sil-1 were grown from a clear synthesis solution containing 40 SiO<sub>2</sub>: 10 TPAOH: 20,000 H<sub>2</sub>O at 403 K for 48 h. The ZSM-5s were crystallized from solutions containing aluminum precursor. Synthesis solutions with composition of 40 SiO<sub>2</sub>: 1.6 Al<sub>2</sub>O<sub>3</sub>: 10 NaOH: 1 TPAOH: 20,000 H<sub>2</sub>O and 40 SiO<sub>2</sub>: 1.2 Al<sub>2</sub>O<sub>3</sub>: 10 NaOH: 1 TPAOH: 20,000 H<sub>2</sub>O were used to prepare the ZSM-5 with Si/Al = 40 and 60, respectively.

Fig. 3 compares the single gas permeances for the three micromembrane units. The figure plots the permeance as a function of the ratio of the kinetic diameter of the diffusing gas molecules to the average pore size of the zeolite (i.e.,  $dp = 5.5 \text{ \AA}$ ). The diffusion of small gas molecules through zeolite pores, as well as the micropores created by the inter-crystalline grain boundaries and imperfections, was primarily Knudsen. The narrow zeolite pore channels constrained the movement of large molecules. The transport of these molecules through the zeolite was strongly influenced by their interaction with the pore wall. Xiao and Wei (1992) calculated that the contribution from configuration diffusion becomes important for ZSM-5 when the size of diffusing molecules exceeds 0.4 nm (i.e.,  $dm/dp = 0.7$ ) and is the dominant transport process as the kinetic diameter of the molecules approaches that of the zeolite pore diameter. Indeed, the general shape of the permeance plots shown in Fig. 3 is similar to the theoretical prediction made by Xiao and Wei (1992).

Table 1 lists some of the reported values of gas permeance in zeolite membranes. The table shows that

the permeability of gases through supported zeolite membranes (i.e., Sil-1 and ZSM-5) varies significantly. The range of permeability values reported for helium ranges from 3 to  $40 \times 10^{-7} \text{ mol}^1 \mu\text{m}^1 \text{ s}^{-1} \text{ m}^{-2} \text{ Pa}^{-1}$  with the most commonly reported value being close to  $10 \times 10^{-7}$ . Hydrogen permeability varies from 10 to  $120 \times 10^{-7} \text{ mol}^1 \mu\text{m}^1 \text{ s}^{-1} \text{ m}^{-2} \text{ Pa}^{-1}$ , while *n*-butane permeability is within  $0.6\text{--}40 \times 10^{-7} \text{ mol}^1 \mu\text{m}^1 \text{ s}^{-1} \text{ m}^{-2} \text{ Pa}^{-1}$ . The most common values for hydrogen and *n*-butane are  $50 \times 10^{-7}$  and  $10 \times 10^{-7} \text{ mol}^1 \mu\text{m}^1 \text{ s}^{-1} \text{ m}^{-2} \text{ Pa}^{-1}$ , respectively. It is often found that membranes with high permeabilities suffer from poor permselectivity due to the presence of a large number of non-zeolite transport pathways in the form of cracks and defects. In contrast, the free-standing zeolite micromembrane units exhibited both high permeability and excellent permselectivity. The permeability of the Sil-1 zeolite micromembranes was nearly an order of magnitude larger with values of  $84.3 \times 10^{-7}$  for helium,  $226.5 \times 10^{-7}$  for hydrogen and  $1.95 \times 10^{-7}$  for *n*-butane. The calculated permselectivities for H<sub>2</sub>/He, H<sub>2</sub>/CH<sub>4</sub> and H<sub>2</sub>/*n*C<sub>4</sub> were 2.7, 0.28 and 116, respectively. Substitution of aluminum in the zeolite framework alters not only the size of the pore channel, but also changes the zeolite chemistry. The addition of aluminum created charge imbalance and transformed the hydrophobic Sil-1 into hydrophilic ZSM-5. Aluminum also imparted the ZSM-5 with both Bronsted and Lewis Acidity. The addition of aluminum led to slower permeation flux (Fig. 3), although the measured permeability is still higher than the literature values (cf. Table 1). In particular, the *n*-butane flux decreased rapidly with increasing aluminum content resulting in higher values of H<sub>2</sub>/*n*C<sub>4</sub> permselectivity. It also resulted in a significant change in the H<sub>2</sub>/CH<sub>4</sub> permselectivity value, which increased from 0.277 to 1.41 with increasing aluminum content (Table 1). The results indicated that the hydrophobic Sil-1 was more selective to methane compared to hydrogen, but as the zeolite became more hydrophilic with the addition of aluminum, the selectivity for methane decreased and the membrane became selective for hydrogen permeation.

Separation was performed using a gas mixture containing 61.7% hydrogen, 12.3% methane and 26.0% carbon dioxide. Table 2 shows that the permeate stream from Sil-1 micromembrane was enriched in methane. The permeate gas contained 52% H<sub>2</sub>, 15.5% CH<sub>4</sub> and 32.5% CO<sub>2</sub>. This is in agreement with the results of the single gas permeation study where the flux of methane through Sil-1 is higher than hydrogen. The strong adsorption of methane on zeolite meant that methane would occupy most of the pore channels, thus restricting the flow of hydrogen. The CO<sub>2</sub> concentration in the permeate outlet was also higher. This suggests that it is possible to concentrate hydrogen in the retentate stream of Sil-1 micromembrane by selective removal of methane and carbon dioxide. This is advantageous since the concentrated hydrogen stream is produced at the higher pressure of the retentate stream. This demonstrates the potential use of the zeolite micromembrane for separation and purification of

Table 1  
Literature data on the gas permeance of MFI membranes

Support	Zeolite thickness S ( $\mu\text{m}$ )	Si/Al	T (K)	Method <sup>a</sup>	Single gas permeance <sup>b</sup> ( $\text{mol}^1 \text{s}^{-1} \text{m}^{-2} \text{Pa}^{-1}$ ) $\times 10^8$					Selectivity		Reference
					He	H <sub>2</sub>	CH <sub>4</sub>	<i>n</i> C <sub>4</sub>	<i>i</i> C <sub>4</sub>	H <sub>2</sub> / <i>n</i> C <sub>4</sub>	<i>n</i> C <sub>4</sub> / <i>i</i> C <sub>4</sub>	
Micromembrane	5	40	298	41 kPa	45	101	72	0.38	—	266.6	—	This work
	5	60	298	41 kPa	88	192	153.7	1.4	—	137.1	—	This work
	5	Sil-1	298	41 kPa	168.6	453	1635	3.88	—	116	—	This work
$\alpha$ -Al <sub>2</sub> O <sub>3</sub> disc	15–20	800	295	He (50 kPa)	—	—	7.1	4.2	0.15	—	28	Xomeritakis et al. (2000) Keizer et al. (1998)
	—	Sil-1	298	He (100 kPa)	—	—	—	1.66	—	—	22–52	
	0.5	Sil-1	298	80 kPa	810	2190	—	98	11	22.34	9.0	Hedlund et al. (2002)
	—	ZSM-5	381	N <sub>2</sub> (101 kPa)	—	—	—	2.7	0.59	—	45	Yan et al. (1997)
	0.5	Sil-1	323	He (101 kPa)	—	—	—	110	37	—	3	Wang et al. (2002)
	0.5	100	323	He (101 kPa)	—	—	—	90	20	—	4.5	Wang et al. (2002)
$\alpha$ -Al <sub>2</sub> O <sub>3</sub> tube	18–50	ZSM5	370	Ar	7.1	—	8.5	12	0.71	—	17.1	Kusakabe et al. (1996) [Fig. 9]
	< 5	12	298	He (100 kPa)	—	—	—	2.8	0.031	—	90	Vroon et al. (1996) [Fig. 8]
	50	300	373	138 kPa	—	46	—	10	1.0	4.6	10	Tuan et al. (1999)
	—	Sil-1	373	dP	72	—	—	46	4.0	—	11.6	Takata et al. (2002)
	9	ZSM-5	293	dP	—	130	—	5.6	0.44	23.21	13	Li et al. (2001)
	—	ZSM-5	408	138 kPa	—	—	—	12	2.0	—	6.2	Coronas et al. (1998) [Figs. 4 & 5]
	2	Sil-1	323	41 kPa	121	313	630	66	1.0	4.74	66	Heng et al. (2004)
	2	66	323	41 kPa	108	303	560	67	0.18	4.52	372	Heng et al. (2004)
	2	16	323	41 kPa	67	204	400	23.6	0.034	8.64	694	Heng et al. (2004)
												Coronas et al. (1997) [Figs. 1 & 2]
$\gamma$ -Al <sub>2</sub> O <sub>3</sub> tube	—	ZSM-5	394	138 kPa	—	—	—	5.4	0.10	—	54	Coronas et al. (1998)
	—	100	300	138 kPa	—	180	—	0.90	0.064	200	14.1	Au and Yeung (2001)
	3	52	323	dP	630	880	—	66.8	140	13.17	0.48	
S.S. disc	30–50	Sil-1	303	He (101 kPa)	—	—	—	3.3	0.13	—	25.4	Van de Graaf et al. (1998)
	35–40	Sil-1	303	He (101 kPa)	—	—	—	6.9–11.9	0.25	—	33–48	Gora et al. (2001)
	50–60	Sil-1	295	He (100 kPa)	30	20	35	4.2	0.072	4.76	58	Bakker et al. (1996)

<sup>a</sup>The reported membrane permeance was measured using pressure or concentration gradient as the driving force.

<sup>b</sup>The values in italics were obtained from butane mixtures.

Table 2  
Gas separation in zeolite micromembranes

Gas mixture	Permeance ( $\text{mol s}^{-1} \text{ m}^{-2} \text{ Pa}^{-1} \times 10^{-7}$ )	Gas ratio (%)			$\text{H}_2/\text{CH}_4$ Sep. ratio
		$\text{H}_2$	$\text{CH}_4$	$\text{CO}_2$	
Feed	—	61.7	12.3	26	
Permeate					
Sil-1	9.64	52.0	15.5	32.5	0.68
ZSM-5 Si/Al = 60	8.36	66.7	12.0	21.3	1.12
ZSM-5 Si/Al = 40	4.26	71.4	9.5	19.1	1.5

hydrogen. It is envisioned that in the future micromembrane units could be used along with a miniature fuel reformer to supply hydrogen to micro-fuel cells.

Gas separation experiments showed that unlike the Sil-1 micromembranes, hydrogen is selectively permeated through the ZSM-5 micromembranes (Table 2). Analysis of the permeate streams for ZSM-5 with Si/Al ratios of 60 and 40 gave gas compositions of 66.7%  $\text{H}_2$ , 12%  $\text{CH}_4$ , 21.3%  $\text{CO}_2$  and 71.4%  $\text{H}_2$ , 9.5%  $\text{CH}_4$ , 19.1%  $\text{CO}_2$ , respectively. This behavior is in accord with the single gas permeation experiment where the flux of hydrogen is greater than methane for the ZSM-5 micromembranes (cf. Table 1 and Fig. 3). It can be speculated that the addition of aluminum weakened the adsorption of methane and carbon dioxide. Indeed, the separation behavior approaches the normal molecular sieving as predicted by the calculations of Xiao and Wei (1992) with higher aluminum content. It is possible to envision the use of ZSM-5 micromembrane in a microreactor for fuel reforming. The selective removal of hydrogen during the reaction is expected to enhance methane conversion and hydrogen yield. We believed that an efficient hydrogen generator could be designed for micro-fuel cell by simply coupling a ZSM-5 membrane microreactor for fuel reforming to a Sil-1 micromembrane separator.

#### 4. Concluding remarks

This work established a fabrication protocol for making zeolite micromembranes. It employed selective seeding and controlled crystallization to incorporate the zeolite into the architecture of the prefabricated silicon substrate. Very precise and localized addition of zeolite materials was achieved, and direct engineering of the deposited zeolite's microstructure and chemistry was also demonstrated. The freestanding zeolite micromembranes possessed good mechanical strength and could withstand normal operating pressures of up to 400 kPa. Further improvement is expected by optimizing the architecture and geometry of the supporting silicon substrate. Low-temperature template removal by ozone prevented the formation of defects and cracks, resulting in zeolite micromembranes that have excellent permeability and permselectivity. This method also led to better membrane reproducibility. Gas permeation and separation

experiments clearly showed that zeolite chemistry plays an important role in membrane transport. Increasing the aluminum content of the zeolite micromembrane results in a large change in membrane selectivity. This suggests that it is possible to achieve different separation targets by careful engineering of the zeolite membrane structure and chemistry.

#### Acknowledgements

We gratefully acknowledge the Hong Kong Research Grant Council (HKUST RGC-HKUST 6021/01P and 6009/02P) and the Institute of Nano Science and Technology for funding this research. We also acknowledge support from the Microelectronics Fabrication Facility (MFF) and Materials Characterization and Preparation Facility (MCPF) of HKUST. We also thank Mr. Siu Ming Kwan for providing some of the SEM pictures.

#### References

- Ajmera, S.K., Jensen, K.F., 2001. Microfabricated packed-bed reactor for phosgene synthesis. *A.I.Ch.E. Journal* 47, 1639–1647.
- Au, L.T.Y., Yeung, K.L., 2001. An investigation of the relationship between microstructure and permeation properties of ZSM-5 membranes. *Journal of Membrane Science* 194, 33–55.
- Bakker, J.W., Kapteijn, F., Poppe, J., Moulijn, J.A., 1996. Permeation characteristics of a metal-supported silicalite-1 zeolite membrane. *Journal of Membrane Science* 117, 57–78.
- Chambers, R.D., Sandford, G., 2001. Elemental fluorine Part 13. Gas-liquid thin film microreactors for selective direct fluorination. *Lab on a Chip* 1, 132–137.
- Coronas, J., Falconer, J.L., Noble, R.D., 1997. Characterization and permeation properties of ZSM-5 tubular membranes. *A.I.Ch.E. Journal* 43, 1797–1812.
- Coronas, J., Noble, R.D., Falconer, J.L., 1998. Separations of  $\text{C}_4$  and  $\text{C}_6$  isomers in ZSM-5 tubular membranes. *Industrial Engineering and Chemical Research* 37, 166–176.
- Cui, T., Fang, J., Zheng, A., Jones, F., Reppond, A., 2000. Fabrication of microreactors for dehydrogenation of cyclohexane to benzene. *Sensors and Actuators B* 71, 228–231.
- Dong, J., Lin, Y.S., Hu, M.Z.-C., Peascoe, R.A., Payzant, E.A., 2000. Template-removal-associated microstructural development of porous-ceramic-supported MFI zeolite membranes. *Microporous Mesoporous Materials* 34, 241–253.
- Gavriilidis, A., Angeli, P., Cao, E., Yeung, K.K., Wan, Y.S.S., 2002. Technology and applications of microengineered reactors. *Chemical Engineering Research and Design* 80, 3–30.

- Geus, E.R., van Bekkum, H., 1995. Calcination of large-MFI-type single crystals 2. Crack formation and thermomechanical properties in view of the preparation of zeolite membranes. *Zeolites* 15, 333–341.
- Gora, L., Nishiyama, N., Jansen, J.C., Kapteijn, F., Teplyakov, V., Mashmeyer, Th., 2001. Highly reproducible high-flux silicalite-1 membranes: optimization of silicalite-1 membrane preparation. *Separation and Purification Technology* 22, 223–229.
- Haswell, S., Skelton, V., 2000. Chemical and biochemical microreactors. *Trac-Trends Analytical Chemistry* 19, 389–395.
- Haswell, S.J., Watts, P., 2003. Green chemistry: synthesis in micro reactors. *Green Chemistry* 5, 240–249.
- Hedlund, J., Sterte, J., Anthonis, M., Bons, A.J., Carstensen, B., Corcoran, N., Cox, D., Deckman, H., Gijst, W.D., Moor, P.P., Lai, F., McHenry, J., Mortier, W., Reinoso, J., Peters, J., 2002. High-flux MFI membranes. *Microporous Mesoporous Materials* 52, 179–189.
- Heng, S., Lau, P.S., Yeung, K.L., Djafer, M., Schrotter, J.-C., 2004. Low-temperature ozone treatment for organic template removal from zeolite membrane. *Journal of Membrane Science* 243, 69–78.
- Hessel, V., Lowe, H., 2003. Microchemical engineering: Components plant concepts user acceptance—Part I. *Chemical Engineering Technology* 26, 13–24.
- Jahnisch, K., Hessel, V., Lowe, H., Baerns, M., 2004. Chemistry in microstructured reactors. *Angewandte Chemie* 43 (4), 406–446.
- Karnik, S.V., Hatalis, M.K., Kothare, M.V., 2003. Towards a palladium micro-membrane for the water gas shift reaction: Microfabrication approach and hydrogen purification results. *Journal of Microelectromechanical Systems* 12, 93–100.
- Keizer, K., Burggraaf, A.J., Vroon, Z.A.E.P., Verweij, H., 1998. Two components permeation through thin zeolite MFI membranes. *Journal of Membrane Science* 147, 159–172.
- Kolb, G., Hessel, V., 2004. Micro-structured reactors for gas phase reactions. *Chemical Engineering Journal* 98, 1–38.
- Kusakabe, K., Yoneshige, S., Murata, A., Morooka, S., 1996. Morphology and gas permeance of ZSM-5-type zeolite membrane formed on a porous  $\alpha$ -alumina support tube. *Journal of Membrane Science* 116, 39–46.
- Kusakabe, K., Morooka, S., Maeda, H., 2001. Development of a microchannel catalytic reactor system. *Korean Journal of Chemical Engineering* 18, 271–276.
- Lai, S.M., Ng, C.P., Marti-Aranda, R., Yeung, K.L., 2003. Knoevenagel condensation reaction in zeolite membrane microreactor. *Microporous Mesoporous Materials* 66, 239–252.
- Li, Y., Zhang, J., Wang, J., Guo, S., 2001. ZSM-5 tubular membranes by varying-temperature synthesis. *Studies in Surface Science and Catalysis* 135, 7–20.
- Madou, M., 1997. *Fundamentals of Microfabrication*, CRC Press, New York.
- Martin, P.M., Matson, D.W., Bennett, W.D., 1999. Microfabrication methods for microchannel reactors and separations systems. *Chemical Engineering Communication* 173, 245–254.
- Quiram, D.J., Jensen, K.F., 2000. Design issues for membrane-based, gas phase microchemical systems. *Chemical Engineering Science* 55, 3065–3075.
- Schiewe, B., Staudt-Bickel, C., Vuin, A., Wegner, G., 2001. Membrane-based gas separation of ethylene/ethylene oxide mixtures for product enrichment in microreactor technology. *Chemical Physics Chemistry* 2, 211–218.
- Takata, Y., Tsuru, T., Yoshioka, T., Asaeda, M., 2002. Gas permeation properties of MFI zeolite membranes prepared by the secondary growth of colloidal silicalite and application to the methylation of toluene. *Microporous Mesoporous Materials* 54, 257–268.
- Tschaufeser, P., Parker, S., 1995. Thermal Expansion Behavior of Zeolites and ALPO<sub>4</sub>s. *Journal of Physical Chemistry* 99, 10609–10615.
- Tuan, V.A., Noble, R.D., Falconer, J.L., 1999. Alkali-free ZSM-5 membranes: preparation conditions and separation performances. *Industrial Engineering and Chemical Research* 38, 3635–3646.
- Van de Graaf, J.M., van der Bijl, E., Stol, A., Kapteijn, F., Moulijn, J.A., 1998. Effect of operating conditions and membrane quality on the separation performance of composite silicalite-1 membranes. *Industrial Chemical Research* 37, 4071–4083.
- Vroon, Z.A.E.P., Keizer, K., Gilde, M.J., Verweij, H., Burggraaf, A.J., 1996. Transport properties of alkanes through ceramic thin zeolite MFI membranes. *Journal of Membrane Science* 113, 293–300.
- Wan, Y.S.S., Gavriilidis, A., Yeung, K.L., 2003. 1-Pentene epoxidation in titanium silicalite-1 microchannel reactor experiments and modelling. *Chemical Engineering Research and Design* 81, 753–759.
- Wang, Z., Hedlund, J., Sterte, J., 2002. Synthesis of thin silicalite-1 film on steel supports using a seeding method. *Microporous Mesoporous Materials* 52, 191–197.
- Worz, O., 2001. Microreactors a new efficient tool for optimum reactor design. *Chemical Engineering Science* 56, 1029–1033.
- Xiao, J., Wei, J., 1992. Diffusion mechanism of hydrocarbons in Zeolites—I. Theory. *Chemical Engineering Science* 47, 1123–1141.
- Xomeritakis, G., Nair, S., Tsapatsis, M., 2000. Transport properties of alumina-supported MFI membrane made by secondary (seeded) growth. *Microporous Mesoporous Materials* 38, 61–73.
- Yan, Y., Davis, M.E., Gavalas, G.R., 1997. Preparation of highly selective zeolite ZSM-5 membranes by a post-synthetic coking treatment. *Journal of Membrane Science* 123, 95–103.